Journal of Materials Chemistry C

Accepted Manuscript

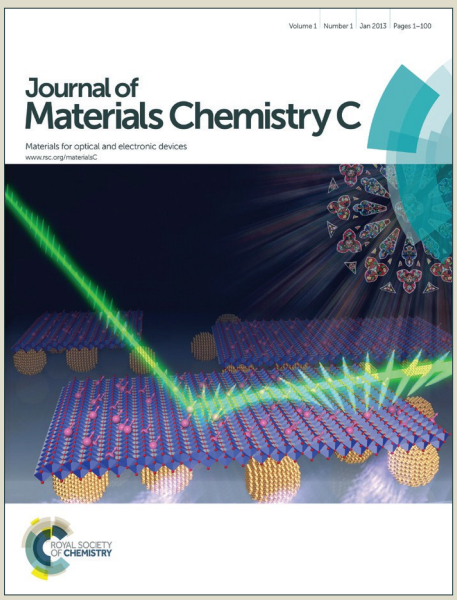

ROYAL SOCIETY OF CHEMISTRY

www.rsc.org/materialsC

Journal Name

RSCPublishing

ARTICLE

A novel fluorescence probe for sensing organic amine vapors from Eu^{3+} β-diketonate functionalized bio-MOF-1 hybrid system

Cite this: DOI: 10.1039/x0xx00000x

Received 00th January 2014,
Accepted 00th January 2014

DOI: 10.1039/x0xx00000x

www.rsc.org/

Xiang Shen, Bing Yan*

A classic anionic metal-organic framework (bio-MOF-1, $Zn_8(ad)_4(BPDC)_6O{\cdot}2Me_2NH_2$ (BPDC = biphenyl-4,4'-dicarboxylate, Ad = adeninate)) encapsulated by Eu^{3+}-β-diketonate complex via cation exchange can be used for sensing volatile organic molecule, especially volatile amines, which is of great significance in environment and industrial monitor. Subsequently, Eu^{3+}-β-diketonate functionalized hybrid system can sensitively detect volatile organic amines and there is a distinct color variation. This means the luminescent intensity of $^5D_0 \rightarrow {}^7F_2$ transition can be significantly enhanced in the basic environment such as diethylamine and dramatically decreased in the acidic environment like formic acid. The color is accompanied by changing from bright red in diethylamine to light purple in formic acid.

Introduction

Metal-organic frameworks (MOFs) have attracted much attention and played more and more significant role in recent years.[1] On one hand, MOFs can be used for gas adsorption based on its own merits of porosity.[2] On the other hand, MOFs can be acted as host material to encapsulate lanthanide ions, dyes or other small molecules via post-synthesis.[3] These functionalized MOFs will have various applications, such as optical devices[4], chemical sensors[4d,5], drug release[6] and catalysts[7]. Among these functionalized MOFs, the luminescent property of lanthanide-functionalized MOFs is an attractive domain.[4d] Thanks to sharp and characteristic emissions, long excited state lifetimes of these trivalent lanthanide ions,[8] these fluorescent MOFs become more promising candidate as luminescent sensors or fluorescent probes.[9] Furthermore, compared to other analytical tools, for example electrochemical devices, fluorescent chemosensor is an expedient detection device with advantages of high signal output, simple detection and low cost.[10]

There are numerous reports on lanthanide-functionalized MOFs as chemical sensors, for instance, ionization sensors,[5b,5c,11] PH sensors[12] and ratiometric thermometers[13]. However, the use of lanthanide complex hosted in MOFs for vapor organic compounds (VOCs) detection has been rarely reported. It is of great significance for detecting VOCs and toxic gases over the last few years because increasing content of these organic molecules have been found in wastewater, industrial monitoring and food safety.[10a,14]

In some previous reports, much success has been achieved in fluorescent probes for basic molecule.[15] For example, europium complexes hosted in nanozeolite L as turn-on sensors have been reported to detect vapor organic amines.[16] However, zeolites have some inherent defects. For instance, it is not allowed zeolites to realize the functionalization of pore surfaces which can be overcome in MOFs, tunable porous materials with modifiable pore surfaces and functionalities.[17] That is to say, a specificity of MOFs is that several structures are highly flexible, as compared to the relatively rigid zeolites. Additionally, MOFs are optical activity whose luminescence consists of $\pi \rightarrow \pi^*$ electron transitions of organic ligands, charge transfer and metal-centered emission.[4d,18] As host materials, several guest molecules such as chromophoric sensitizers and lanthanide ions can be incorporated into the structures via post-synthesis and tailored to modulate and optimize the photoluminescence properties of lanthanide cations through antenna effect.[19,20] Therefore, lanthanide-functionalized MOFs will have multiple luminescent centers and display various colors. Based on this, they can be employed as fluorescent sensors with color variation.

In this report, a simple and convenient strategy for synthesizing a fluorescent sensor to detect and discriminate the types of organic amines vapors is presented. Several papers have reported that the self-assembly of europium ions with β-diketonate or lewis bases is driven by the pH value of the surrounding environment which will have a significant impact on the Eu^{3+} characteristic luminescence.[12] Inspired by these research, an anionic MOF (bio-MOF-1, $(Zn_8(ad)_4(BPDC)_6O{\cdot}2Me_2NH_2$, BPDC = biphenyl-4,4'-dicarboxylate, Ad = adeninate)) is selected where the cationic guest molecules or ions can undergo facile exchange with other exogenous cationic species. Further, the β-diketonate (thenoyltrifluoroacetonate, TTA) as second sensitized ligand can effectively sensitize the

luminescence of Eu^{3+}-doped MOF.[21] It is a robust platform to realize the detection of organic amines vapors which displays bright red emission in the basic environment while shows light purple in the acidic environment. The innovation of this chemosensor is color variations at different organic vapors.

Experimental section

Chemicals. All chemicals were purchased from commercial sources and used without purification. Europium nitrate was obtained by dissolving corresponding oxide in nitric acid, followed by evaporation and vacuum drying. Biphenyl-4,4'-dicarboxylic acid (BPDC), adenine and 2-thenoyltrifluoroaceton (TTA, 99 %) were purchased from Adamas-beta. N, N'-dimethylformamide (DMF, 99.9 %) was from Aladdin. Zinc acetate dehydrate and nitric acid was purchased from China National Medicine Group. Ultrapure water and ethanol were used throughout all experiment.

Synthesis of bio-MOF-1(1).[6a,19] Adenine (0.125 mmol), BPDC (0.25 mmol), zinc acetate dehydrate (0.375 mmol), nitric acid (1 mmol), DMF (13.5 mL), and water (1 mL) were added to a Teflon-lined autoclave, heated at 130 °C for 24 h, and then cooled to room temperature naturally. The material was collected, washed with DMF (5 mL × 3), and dried under vacuum (24 h).

Preparation of $Eu^{3+}_{0.005}$@1.[19a] The lanthanide cation was performed by cation exchange. The compound **1** (135 mg, 0.04 mmol), solution of $Eu(NO_3)_3{\cdot}6H_2O$ in the DMF(4 mL, 0.05 mmol·L^{-1}) and DMF (10 mL) were added to a Teflon capped 20 mL scintillation vial and heated on a hotplate at 50 °C for 24 hrs. Finally, the products were washed using water and DMF solvents. ICP analysis showed that the molar ration of Zn^{2+}/Eu^{3+} was 1: 0.0048.

Preparation of $Eu^{3+}_{0.005}$-TTA@1(2).[19b] In order to introduce TTA into Eu^{3+}@**1**, we use a synthetic method called the gas diffusion method, similar to modified zeolite. Eu^{3+}@**1** (30 mg) was kept in the vapour of TTA (150 mg) at 50 °C for 12 hrs, ensuring that one europium ion can completely react with three TTA molecules to build a six-membered chelate. The temperature depends on the temperature of sublimation of TTA. The resulting material was washed with acetonitrile to remove residual Ln^{3+} caiton and TTA molecule, centrifuged twice and TTA molecule and finally dried at 80 °C under normal atmospheric conditions. Finally, the products were washed using water and DMF solvents. ICP analysis showed that the molar ration of Zn^{2+}/Eu^{3+} was 1: 0. 004.

Exposure to various solvent.[10a,16] Powder samples of **2** were used for sensing experiments and the setup is shown in Figure S6. 10mg of **2** was put in a small bottle and exposed to various solvent vapours. Both were placed into a sealed container, containing about 3 mL of solvent for 1 h. The luminescence spectra of **2**, before and after exposed to the solvent vapours, were measured.

Physical characterization. X-ray powder diffraction patterns (XRD) were recorded with a Bruker Foucs D8 at 40kV, 40mA for Cu-Kα with a scan speed of 0.10 sec/step and a step size of 0.02 °; the data were collected within 2θ range of 3-50 °. Scanning electronic microscope (SEM) images were obtained with a Hitachi S-4800. Fourier transform infrared spectra (FTIR) were measured with KBr slices from 4000 to 400 cm^{-1} using a Nexus 912AO446 infrared spectrum radiometer. Thermogravimetric analysis (TGA) was measured using a Netzsch STA 449C system at a heating rate of 15 K min^{-1} under nitrogen atmosphere. UV-Vis spectra were recorded on Agilent 8453. The measurement of metal ion was performed on Agilent 7700X inductively coupled plasma-mass spectrometer (ICPMS).

Luminescent measurements. The luminescence spectra were recorded on an Edinburgh FL920 phosphorimeter using a 450W xenon lamp as excitation source. Luminescence lifetime measurements are carried out on an Edinburgh FLS920 phosphorimeter using a microsecond pulse lamp as excitation source. The quantitative value of lifetime is calculated by linear fitting.

Results and Discussion

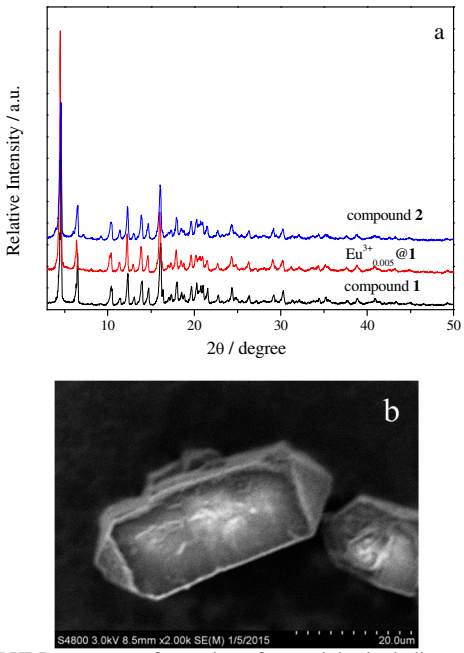

Figure 1 PXRD patterns of a series of materials, including compound **1**, $Eu^{3+}_{0.005}$@**1** and **2** (a) and SEM image of **2** (b)

Bio-MOF-1(**1**) is hydrothermally synthesized according to the previous report which consists of infinite zinc-adenine columnar secondary building units and these columns are interconnected via multiple BPDC linkers.[6a,19] What's more, compound **1** is anionic and dimethylammonium (DMA) cations reside in its pores. Based on this, $Eu^{3+}_{0.005}$-TTA@**1** **(2)** is prepared by a post-synthesis method. Firstly, as compound **1** can serve as both a host and an antenna for protecting and sensitizing extra-framework lanthanide cations, europium ions are encapsulated within the MOF pores via cation exchange.[18a] Secondly, according to the results of the forefathers, compound **1** is a crystalline porous material with two types of one-dimensional channels along the c axis of about 7× 7 and 10 × 10 Å^2.[3c] Thereafter, some small molecule such as TTA (2-thenoyltrifluoreacetonate, shown in Figure S1) could encapsulate into the pores as well to further sensitize Eu^{3+} ions. When TTA encapsulating into the framework, not only the photostability but also the thermostability have been improved. (Figure S2) TG

analysis of **1** indicates that a weight loss of 20 % from 100 °C to 250 °C, which can be attributed to the loss of water molecule and dimethylammonium cations. Thereafter, a further mass loss can be observed, caused by the decomposition of the framework. However, only a small weigh loss of 5% prior to decomposition can be observed of compound **2** after introducing TTA, which indicates this material has a fine thermal stability. Additionally, the X-ray diffraction patterns (Figure 1a) and SEM image (Figure 1b) demonstrate that there were no significant changes in the framework and the crystallization is still intact after post-synthesis. The FT-IR spectra (Figure S3) can successfully demonstrate the coordination of Eu^{3+} ions and TTA as well as the framework. HTTA has vibration at around 1652 cm^{-1} belong to C=O vibration. When introducing TTA into the framework, the C=O stretching vibration of TTA has changed to 1670 cm^{-1} and the asymmetric vibrations of carboxylate ions of the compound **1**. And the absorbance band at 1540 cm^{-1} is ascribe to the C=C stretching vibrations of the TTA ligand.[16] Moreover, characteristic peaks of benzene ring stretching vibration at 1600 cm^{-1} from the framework remains after the reaction.

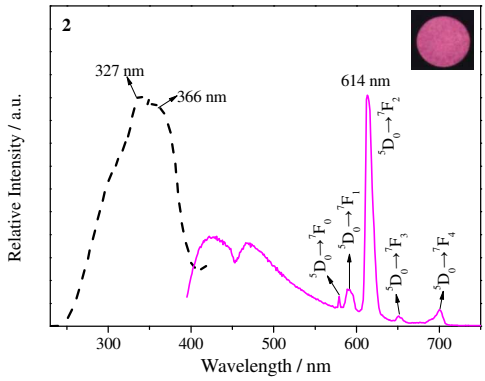

Figure 2 The excitation (dotted line) and emission (solid line) spectra of compound **2** (λ_{ex} = 366 nm, λ_{em} = 614 nm) and the inset is photograph of compound **2** under UV lamp (365 nm) showing the colour is magenta.

The luminescent properties of three materials, including **1**, $Eu^{3+}_{0.005}$@**1** and **2** are investigated and the results are shown in Figure S4, S5 and Figure 2 respectively. For the emission spectrum of $Eu^{3+}_{0.005}$@**1** (Figure S5), only the characteristic Eu(III) emission occurring at 593, 614 and 700 nm for the deactivation of the $^5D_0$ excited state to ^7F_J (J = 1, 2, 4) under excitation at 327 nm can be observed. Besides, an intense broad band at around 400 nm is considered to the host, namely compound **1**. To prove this, the luminescent spectrum of compound **1** is measured in Figure S4. The broad band at around 398 nm is due to $\pi\rightarrow\pi^*$ electron transitions of organic ligands when excited at 332 nm. With TTA encapsulating into the framework, the emission spectrum changes clearly. For one thing, another two peaks of Eu^{3+} characteristic transitions at 579 and 650, which belongs to $^5D_0\rightarrow{}^7F_J$ (J = 0, 3), can be observed as well under the excitation at 327 nm. For another, compound **2** exhibits not only all the Eu^{3+} characteristic peaks assigned to f-f electronic transitions but also the emission of compound **1**, a broad band from 400 nm to 500 nm. The excitation spectrum of **2** is obtained by monitoring the emission wavelength at 614 nm. Generally, the excitation wavelength of a trivalent lanthanide ion greatly depends on the ligands, which is so called antenna effect. However, the excitation spectrum in Figure 2 is dominated by two bands centered at 327 nm and 366 nm. Compared with the excitation spectrum of single Eu^{3+}-doped sample, the band at 327 nm could be chiefly assigned to the excitation of compound **1** and the band at 366 nm should mostly belong to the excitation of TTA energy absorption. It proves TTA has loaded into the porous successfully. Insets in Figure S5 and Figure 2 are luminescent photographs of $Eu^{3+}_{0.005}$@**1** and **2**, respectively. Under UV light irritation of 365 nm, $Eu^{3+}_{0.005}$@**1** displays blue while compound **2** emits magenta after sensitized by the second sensitized ligand.

Further, the luminescence sensing measurements are performed to investigate the influence of different guest molecules. The sample is exposed to various volatile organic molecules for 1 h and the results are shown in Figure S7 and Figure 3. The feature is that the intensities in the photoluminescent spectra (Figure S7) are strongly dependent on the solvent molecules, particularly in the case of basic molecules such as ammonia and ethylenediamine, which exhibit the significant enhancement effect. Histogram in Figure 3a shows the luminescent enhancement spectra of $^5D_0\rightarrow{}^7F_2$ transition at 614 nm upon exposure to several solvent molecules vapours. A remarkable enhancement in luminescence intensity can be observed for vapours of NH_3 and ethylenediamine. The luminescent intensity of **2**-NH_3 is more than three times stronger than **2**. **2**-$C_2H_8N_2$ has similar phenomenon, whose emission intensity is about 2.7 times stronger than that of the origin one. For other solvent molecules such as ethanol, acetone, acetonitrile, less than a twofold enhancements could be observed. There is a little quench of the intensity in the water vapour because water can quench the lanthanide excited state through O-H vibration deactivation.[22] Furthermore, the boost in luminescence of **2** is easily visible upon UV-light irritation at 365 nm by naked eyes, shown in Figure S8. Theoretically, colours of all materials have been marked through the calculation from the CIE diagram chromaticity in Figure 3b. Different letters represent different solvents, especially, d for compound **2**, l for **2**-$C_2H_8N_2$ and m for **2**-NH_3. It is evident that the colour of **2** has shifted toward redness in the alkaline atmosphere. The detailed CIE coordinates are listed in Table S1. Moreover, it seems that this trend follows some regulations, which means vapours with certain features such as organic amine vapours, are likely to boost the luminescence.

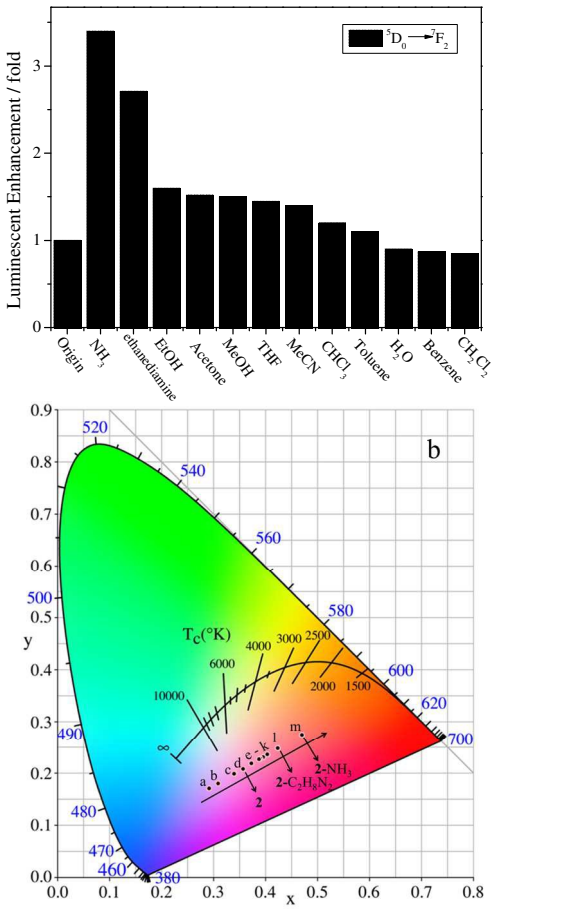

Figure 3 (a) Histogram of an enhancement in the emission intensity of $^5D_0 \rightarrow {}^7F_2$ transition at 614 nm after exposure to vapours of various organic molecule solvents. (b) The CIE diagram chromaticity of compound **2** upon contact with corresponding vapours. (Different letters represent different solvents, seeing in Supporting Information.)

A series of organic amines and one kind of organic acid are selected in order to further study the luminescent trend and inherent mechanism.(Figure 4a) The enhancement in emission intensity by a factor of 14, 9 and 4 for vapours of diethylamine ($(C_2H_5)_2NH$), triethylamine (Et_3N) and NH_3, respectively, whereas an intense quench occurred when exposed to formic acid (FA). Another interesting phenomenon in the embedded luminescent spectrum in Figure 4a is that the formic acid only quenches the characteristic emission of europium ions while the emission of the host material retains. The digital photographs of theses samples in the insets of Figure 4a have changed accordingly. It is visual that the colour has shifted from bright red in diethylamine to pink in NH_3 and then light purple in the acidic environment under UV excitation of 365 nm. A detailed colour change is shown in Figure 4b in CIE diagram chromaticity. The CIE diagram coordinate of compound **2** is (0.3739, 0.2183) that transfers to (0.5965, 0.3289) in the diethylamine vapours while shifts to (0.203, 0.1334) in the formic acid atmosphere. It is important to note that compound **2**, as a sensing material, has great potency to discrimination whether the surrounding environment is acidic or alkaline based on colour switching.

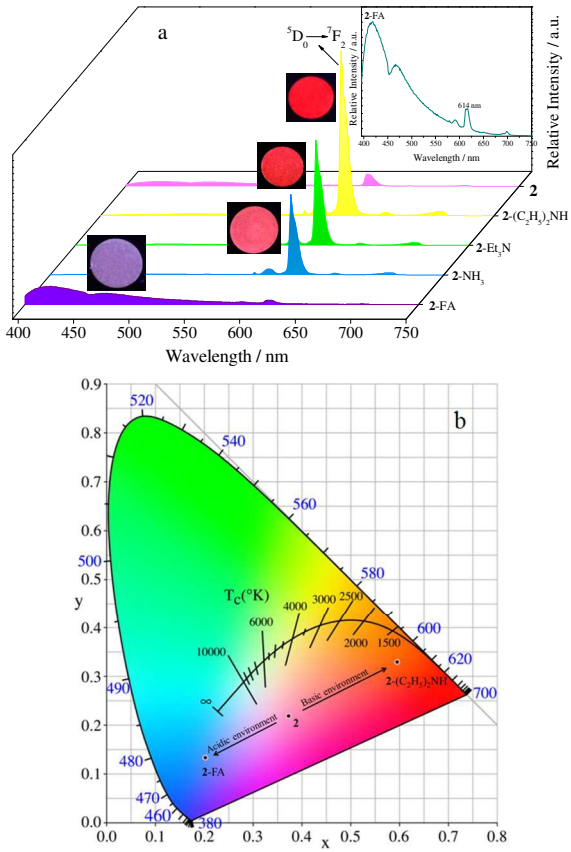

Figure 4 (a) The luminescent spectra of compound **2** when exposed to vapours of three kinds of organic amines such as $(C_2H_5)_2NH$, Et_3N, NH_3 and one kind of organic acid, formic acid. The embedded emission spectrum is an enlarged spectrum of **2**-FA from 400 nm to 750 nm and four digital photos of compound **2** after contact with corresponding vapours under UV irradiation of 365 nm. (b) The CIE diagram chromaticity of compound **2** (x = 0.3739, y = 0.2183), **2**-$(C_2H_5)_2NH$ (x = 0.5965, y = 0.3289) and **2**-FA (x = 203, y = 0.1334).

The sensing mechanism of Eu^{3+} complex with TTA is discussed as follows. Eu^{3+} ions inside the channels of **1** can be coordinated with TTA to build six-membered chelate ring. However, H^+ proton could break this chelate ring because TTA ligand could be protonated in the acidic environment. This protonation effect can impair the sensitization of β-diketonate to Eu^{3+}. As a result, the luminescence intensity of Eu^{3+} would be quenched instantaneously.[12a,16] In other words, the basic organic amines are beneficial to the formation of Eu^{3+}-β-diketonate complex with high coordination numbers while incomplete coordination due to protonation is detrimental to the luminescence. Several previous reports have been reported β-diketonate in the alkaline environment could coordinate with Eu^{3+} ions and sensitize its luminescence.[12b,23] The interpretation of this mechanism is also supported by the Judd-Ofelt theory[24], the intensity ratio of $^5D_0 \rightarrow {}^7F_2$ to $^5D_0 \rightarrow {}^7F_1$. The intensity ratio $I(^5D_0 \rightarrow {}^7F_2)/I(^5D_0 \rightarrow {}^7F_1)$ is a significant parameter to probe the symmetry of Eu^{3+} coordination sites, which indicates the Eu^{3+} coordination environment changes as the ratio altered. Values of the intensity ratio $I(^5D_0 \rightarrow {}^7F_2)/I(^5D_0 \rightarrow {}^7F_1)$ as well as corresponding lifetimes are shown in Table 1. It reveals that the ratio of **2** is only 8.7 while it increases to 13.31, 12.49, 12.30 after exposed to vapours of

$(C_2H_5)_2NH$, Et_3N and NH_3, respectively. The ratios are very close to each other upon contact with three kinds of amines and reflect europium ions have the similar coordination mode. That is to say, this implies there is a complete coordination between Eu^{3+} and β-diketonate in the basic environment. To the contrary, the ratio has declined to 6.57 upon exposure to formic acid that means H^+ proton break the coordination. The UV-Vis spectrum in Figure S9 could improve this point once again. The absorption has transferred after exposure to formic acid while others have no obvious change. As shown in Table 1 and Figure S10, the lifetime curves are well represented by a bi-exponential function and the variation order of lifetime data is in good agreement with that of the luminescent intensity. Furthermore, a phenomenon could be observed that the order of luminescence boost for the selected amines is by the sequence of $(C_2H_5)_2NH > Et_3N > NH_3$, which is fully in accordance with the trend of the pK_a of the corresponding conjugate acids.

Table 1 Photophysical data of several materials about lifetimes and the intensity ratios of $I(^5D_0\rightarrow{}^7F_2)/ I(^5D_0\rightarrow{}^7F_1)$

Sample	τ (μs)	$I(^5D_0\rightarrow{}^7F_2)/ I(^5D_0\rightarrow{}^7F_1)$
2	166.55	8.7
2-$(C_2H_5)_2NH$	595.46	13.31
2-Et_3N	484.57	12.49
2-NH_3	360.42	12.30
2-FA	46.72	6.57

Moreover, a deep research has made to discuss the properties of samples after sensing. The structure of compound **2** is almost stable at different volatile organic solutions, which is confirmed by PXRD in Figure S11. The TGA plot ensures to check the organic vapours inside the pore. Compared with the TG data in Figure S1, a weight loss of about 24 % from room temperature to 400 °C could be observed in Figure S12, which is considered to the loss of organic solvents in the pores gradually. A further mass loss is caused by the decomposition of the framework after 400 °C. It is evidence that organic small molecule has loaded into the pores as well as the frameworks are intact after sensing researches.

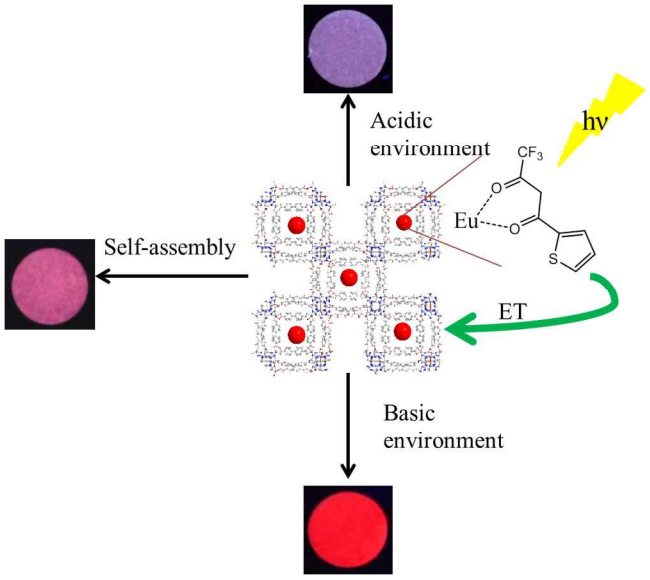

Figure 5 Schematic representation of the fluorescence sensor based on bio-MOF-1. The self-assembled material, compound **2**, displays the colour of magenta. H^+ protons could break the chelate ring between Eu^{3+} and TTA and impair the sensitization of TTA to Eu^{3+}. The colour transfers to blue which belongs to the luminescence of the host in the acidic environment. And diethylamine including other organic amines could recover the sensitization with the colour changing to bright red.

Based on the above research, a kind of fluorescence probe of sensing organic amines could be designed as shown in Figure 5. Here the Eu^{3+} emission changes are visible under the UV lamp. A slight amount of Eu^{3+} and TTA has self-assembled into MOFs displaying the colour is magenta. The ICP analysis showed that the molar ration of Zn^{2+}/Eu^{3+} is 1:0.004 in the compound **2** with the purpose of economy and environmental friendly. Thanks to the advantages of MOFs, we can intuitively distinguish the acid-base property in the surrounding environment through the colour variation. The enhancing bright red fluorescence emission is observed when in alkaline volatile organic molecule, particularly diethylamine, while the assembly dissociated and the material displays light purple fluorescence emission in acidic vapour, such as formic acid.

Conclusion

In summary, a fluorescent sensor is designed to selectively detect organic amines vapors among several volatile organic solutions. This sensor is based on the encapsulation of Eu^{3+}-β-diketonate complexes within a metal-organic framework. Two key points of note are that europium ions are encapsulated into the channel via cations exchange which is a simple post-synthesis method and that the amount of europium ions is very slight in purpose of economy. There is a remarkable enhancement in characteristic emission of Eu3+ at 614 and a long lifetime of Eu^{3+} ions when exposed to organic amines vapors. Dramatically quench in luminescent emission and in lifetimes occurred in the acidic vapors while the host luminescence of bio-MOF-1 still exists. As a result, a concomitant phenomenon is color switching. We can discriminate basic molecule vapors though the bright red color and tell acidic vapors via light purple. Meanwhile, the mechanism responsible for the luminescent

response is discussed as well as the samples' properties after sensing. It is believable that this sensor has various desirable properties and is a cost-effectiveness sensing material.

Acknowledgements

This work is supported by the National Natural Science Foundation of China (91122003) and Developing Science Funds of Tongji University.

Notes and references

Department of Chemistry, Tongji University, Shanghai 200092, P. R. China. E-mail: byan@tongji.edu.cn

† Electronic Supplementary Information (ESI) available: Experimental, synthesis and characterization details. See DOI: 10.1039/b000000x/

1. (*a*) H. C. Zhou, J. R. Long and O. M. Yaghi, *Chem. Rev.*, 2012, **112**, 673; (*b*) A. U. Czaja, N. Trukhan and U. Muller, *Chem. Soc. Rev.*, 2009, **38**, 1284; (*c*) J. R. Li, J. Sculley and H. C. Zhou, *Chem. Rev.*, 2011, **112**, 869.
2. (*a*) Z. Wang, H. Sezen, J. Liu, C. Yang, S. E. Roggenbuck, K. Peikert, M. Fröba, A. Mavrantonakis, B. Supronowicz, T. Heine, H. Gliemann and C. Wöll, *Micropor. Mesopor. Mater.*, 2015, **207**, 53; (*b*) K. Liu, B. Li, Y. Li, X. Li, F. Yang, G. Zeng, Y. Peng, Z. Zhang, G. Li, Z. Shi, S. Feng and D. Song, *Chem. Commun.*, 2014, **50**, 5031; (*c*) E. Tsivion, J. R. Long and M. Head-Gordon, *J. Am. Chem. Soc.*, 2014, **136**, 17827.
3. (*a*) Y. Lu and B. Yan, *J. Mater. Chem. C*, 2014, **2**, 5526; (*b*) Y. Zhou and B. Yan, *Inorg. Chem.*, 2014, **53**, 3456; (*c*) J. C. Yu, Y. J. Cui, H. Xu, Y. Yang, Z. Y. Wang, B. L. Chen and G. D. Qian, *Nat. Commun.*, 2013, 4, 2179.
4. (*a*) Y. Zhou and B. Yan, *Nanoscale*, 2015, **7**, 4063; (*b*) Y. Lu and B. Yan, *Chem. Commun.*, 2014, **50**, 15443; (*c*) C. Y. Sun, X. L. Wang, X. Zhang, C. Qin, P. Li, Z. M. Su, D. X. Zhu, G. G. Shan, K. Z. Shao, H. Wu and J. Li, *Nat. Commun.*, 2013, 4; (*d*) Y. J. Cui, Y. F. Yue, G. D. Qian and B. L. Chen, *Chem. Rev.*, 2012, **112**, 1126.
5. (*a*) X. Shen and B. Yan, *RSC Adv.*, 2015, **5**, 6752; (*b*) J. N. Hao and B. Yan, *J. Mater. Chem. A*, 2014, **2**, 18018; (*c*) X. Y. Xu and B. Yan, *Acs. Appl. Mater. Inter.*, 2014, **7**, 721; (*d*) R. Wang, X. Y. Dong, H. Xu, R. B. Pei, M. L. Ma, S. Q. Zang, H. W. Hou and T. C. W. Mak, *Chem. Commun.*, 2014, **50**, 9153.
6. (*a*) J. Y. An, S. J. Geib and N. L. Rosi, *J. Am. Chem. Soc.*, 2009, **131**, 8376; (*b*) K. Matsuyama, N. Hayashi, M. Yokomizo, T. Kato, K. Ohara and T. Okuyama, *J. Mater. Chem. B*, 2014, **2**, 7551; (*c*) T. Kundu, S. Mitra, P. Patra, A. Goswami, D. D. Diaz and R. Banerjee, *Chem-Eur. J.*, 2014, **20**, 10514; (*d*) J. Della Rocca, D. M. Liu and W. B. Lin, *Accounts Chem. Res.*, 2011, **44**, 957.
7. (*a*) I. Hod, W. Bury, D. M. Gardner, P. Deria, V. Roznyatovskiy, M. R. Wasielewski, O. K. Farha and J. T. Hupp, *J. Phys. Chem. Lett.*, 2015, 586; (*b*) A. Dhakshinamoorthy, M. Alvaro and H. Garcia, *Chem. Commun.*, 2012, **48**, 11275.
8. (*a*) B. Yan, *RSC Adv.*, 2012, **2**, 9304; (*b*) J. C. G. Bunzli and C. Piguet, *Chem. Soc. Rev.*, 2005, **34**, 1048; (*c*) L. D. Carlos, R. A. S. Ferreira, V. D. Bermudez and S. J. L. Ribeiro, *Adv. Mater.*, 2009, **21**, 509.
9. (a) L. V. Meyer, F. Schonfeld and K. Muller-Buschbaum, *Chem. Commun.*, 2014, **50**, 8093; (*b*) S. V. Eliseeva and J. C. G. Bunzli, *Chem. Soc. Rev.*, 2010, **39**, 189.
10. (a) J. Chen, F. Y. Yi, H. Yu, S. Jiao, G. Pang and Z. M. Sun, *Chem. Commun.*, 2014, **50**, 10506; (*b*) L. Basabe-Desmonts, D. N. Reinhoudt and M. Crego-Calama, *Chem. Soc. Rev.*, 2007, **36**, 993.
11. Y. Zhou, H.-H. Chen and B. Yan, *J. Mater. Chem. A*, 2014, **2**, 13691.
12. (*a*) Y. Lu and B. Yan, *Chem. Commun.*, 2014, **50**, 13323; (*b*) J. P. Leonard, C. M. G. dos Santos, S. E. Plush, T. McCabe and T. Gunnlaugsson, *Chem. Commun.*, 2007, 129.
13. (*a*) X. T. Rao, T. Song, J. K. Gao, Y. J. Cui, Y. Yang, C. D. Wu, B. L. Chen and G. D. Qian, *J. Am. Chem. Soc.*, 2013, **135**, 15559; (*b*) Y. J. Cui, H. Xu, Y. F. Yue, Z. Y. Guo, J. C. Yu, Z. X. Chen, J. K. Gao, Y. Yang, G. D. Qian and B. L. Chen, *J. Am. Chem. Soc.*, 2012, **134**, 3979; (*c*) Y. Zhou, B. Yan and F. Lei, *Chem. Commun.*, 2014, **50**, 15235.
14. (*a*) A. Fekete, A. K. Malik, A. Kumar and P. Schmitt-Kopplin, *Crit. Rev. Anal. Chem.*, 2010, **40**, 102; (*b*) V. P. Aneja, P. A. Roelle and G. C. Murray, *Atmos. Environ.*, 2001, **35**, 1903.
15. (*a*) X. Zhang, X. Liu, R. Lu, H. Zhang and P. Gong, *J. Mater. Chem.*, 2012, **22**, 1167; (*b*) R. Haldar, R. Matsuda, S. Kitagawa, S. J. George and T. K. Maji, *Angew. Chem. Int. Edit.*, 2014, **53**, 11772; (*c*) Y. Fu, J. Yao, W. Xu, T. Fan, Q. He, D. Zhu, H. Cao and J. Cheng, *Polymer Chemistry*, 2015, **6**, 2179; (*d*) J. Roales, J. M. Pedrosa, M. G. Guillén, T. Lopes-Costa, S. M. A. Pinto, M. J. F. Calvete and M. M. Pereira, *Sensors Actuators B: Chem.*, 2015, **210**, 28; (*e*) P. Xue, Q. Xu, P. Gong, C. Qian, A. Ren, Y. Zhang and R. Lu, *Chem. Commun.*, 2013, **49**, 5838; (*f*) S. Rochat and T. M. Swager, *Angew. Chem. Int. Edit.*, 2014, **53**, 9792.
16. P. Li, Y. Z. Zhang, Y. G. Wang, Y. J. Wang and H. R. Li, *Chem. Commun.*, 2014, **50**, 13680.
17. D. Peralta, G. Chaplais, A. Simon-Masseron, K. Barthelet, C. Chizallet, A. A. Quoineaud and G. D. Pirngruber, *J. Am. Chem. Soc.*, 2012, **134**, 8115.
18. M. D. Allendorf, C. A. Bauer, R. K. Bhakta and R. J. T. Houk, *Chem. Soc. Rev.*, 2009, **38**, 1330.
19. (a) J. Y. An, C. M. Shade, D. A. Chengelis-Czegan, S. Petoud and N. L. Rosi, *J. Am. Chem. Soc.*, 2011, **133**, 1220; (b) B. Y. Li, Y. M. Zhang, D. X. Ma, T. L. Ma, Z. Shi and S. Q. Ma, *J. Am. Chem. Soc.*, 2014, **136**, 1202; (c) T. Li and N. L. Rosi, *Chem. Commun.*, 2013, **49**, 11385; (d) J. An and N. L. Rosi, *J. Am. Chem. Soc.*, 2010, **132**, 5578.
20. K. Binnemans, *Chem. Rev.*, 2009, **109**, 4283.
21. (*a*) X. Shen and B. Yan, *Journal of Colloid and Interface Science*, 2015, **451**, 63; (*b*) Y. X. Ding, Y. G. Wang, H. R. Li, Z. Y. Duan, H. H. Zhang and Y. X. Zheng, *J. Mater. Chem.*, 2011, **21**, 14755.
22. (*a*) S. Faulkner and B. P. Burton-Pye, *Chem. Commun.*, 2005, 259; (*b*) M. P. Lowe and D. Parker, *Chem. Commun.*, 2000, 707.
23. (*a*) J. N. Hao and B. Yan, *Dalton Trans.*, 2014, **43**, 2810; (*b*) J. N. Hao and B. Yan, *New J. Chem.*, 2014, **38**, 3540.
24. L. Fu, R. A. S. Ferreira, N. J. O. Silva, A. J. Fernandes, P. Ribeiro-Claro, I. S. Goncalves, V. d. Z. Bermudez and L. D. Carlos, *J. Mater. Chem.*, 2005, **15**, 3117.

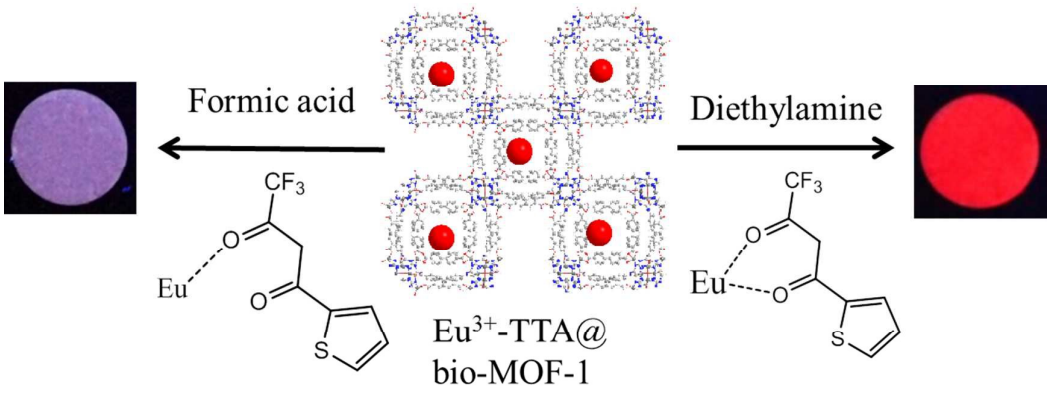

A classic anionic metal-organic framework (bio-MOF-1) for Eu^{3+}-β-diketonate complex encapsulation via post-synthesis has the utility of sensory material for sensing volatile organic molecule, especially volatile amines, which is of great significance in environment and industrial monitor. The β-diketonate as second sensitized ligand can effectively sensitize the luminescence of Eu^{3+}-doped MOF. Subsequently, Eu^{3+}-β-diketonate functionalized sample could sensitively detect volatile organic amines and there is a distinct color variation. This means the luminescent intensity of $^5D_0 \rightarrow {}^7F_2$ transition can be significantly enhanced in the basic environment such as diethylamine and dramatically decreased in the acidic environment like formic acid. The color is accompanied by changing from bright red in diethylamine to light purple in formic acid.